Journal of Molecular Catalysis A: Chemical 300 (2009) 116–120

Contents lists available at ScienceDirect

Journal of Molecular Catalysis A: Chemical

journal homepage: www.elsevier.com/locate/molcata

In situ formation of $HRh(CO)_2(PPh_3)_2$ active species on the surface of a SBA-15 supported heterogeneous catalyst and the effect of support pore size on the hydroformylation of propene

Li Yan[a], Yun J. Ding[a,b,*], Li W. Lin[a,b], He J. Zhu[a], Hong M. Yin[a], Xian M. Li[a], Yuan Lu[a]

[a] Laboratory of Applied Catalysis, Dalian Institute of Chemical Physics, Chinese Academy of Sciences, Dalian, Liaoning 116023, China
[b] The State Key Laboratory of Catalysis, Dalian Institute of Chemical Physics, Chinese Academy of Sciences, Dalian, China

ARTICLE INFO

Article history:
Received 30 April 2008
Received in revised form 30 October 2008
Accepted 30 October 2008
Available online 17 November 2008

Keywords:
Triphenyl phosphine
Rh
SBA-15
Hydroformylation
Propene

ABSTRACT

A method of in situ formation of $HRh(CO)_2(PPh_3)_2$ active species on the surface of heterogeneous Rh/SBA-15 catalyst has been developed and confirmed in this work. The amount of active species formed inside the pores can be controlled by the support pore size. This class of PPh_3-Rh/SBA-15 catalyst has been employed in propene hydroformylation to be highly active, selective, stable, easily workable and recyclable. Using TEM, solid-state ^{31}P MAS NMR, and in situ FT-IR, $HRh(CO)_2(PPh_3)_2$ active species can be characterized.

1. Introduction

Rh-catalyzed hydroformylation has received a great deal of attention from both academia and industry, and it is one of the most thoroughly investigated reactions in homogeneous catalysis [1]. Current efforts in hydroformylation research are focused mainly on versatile methods of immobilization or heterogenizing homogeneous catalysts, and biphasic catalysis, including the utilization of ionic liquids and supercritical fluids [2]. Although many approaches show considerable promise, key problems for many systems are catalyst stability, leaching of catalytic material into the product phase, and the cost of the catalyst, ligand, solvent, or process [2].

Recently, we have reported that PPh_3 modified heterogeneous Rh/SiO_2 is a new important class of heterogeneous catalyst (PPh_3-Rh/SiO_2) with high efficiency and stability for hydroformylation, and which is a combination of homogeneous and heterogeneous catalysts [3,4]. Though many studies confirm that Rh(0) nano-particles can transform into mononuclear or multinuclear complexes under reaction condition, which are responsible for the catalytic activity [5–8], the results still raise the important questions of how the Rh-phosphine carbonyl complexes form on the surface of heterogeneous catalyst and how to control the active species. Therefore, we employed SBA-15 (S15) as a support in PPh_3-Rh/S15 system. Since S15 has a hexagonal array of uniform mesopores with controllable pore size and more than 98% of the total surface area is the well defined area inside the pores [9], it offers new opportunities to elucidate the structure, bonding, and interaction between Rh and triphenyl phosphine. We found that pore size has a remarkable effect on the in situ formation of Rh-phosphine carbonyl complexes.

2. Experimental

It is well known that phosphines are very sensitive to water or oxygen, and they can easily be oxidized under such conditions and then lose their catalytic activity. Considering these facts, all manipulations were routinely performed under an argon atmosphere using standard Schlenk techniques.

2.1. Synthesis of the Rh/S15, PPh_3-Rh/S15 and $HRh(CO)(PPh_3)_3$/S15 catalysts

All catalysts were prepared using commercial SBA-15 (S15) (Jilin University High-Tech. Co. Ltd.) as supports. The S15 powder was

* Corresponding author at: Laboratory of Applied Catalysis, Dalian Institute of Chemical Physics, Chinese Academy of Sciences, Dalian, Liaoning 116023, China. Tel.: +86 411 84379143; fax: +86 411 84379143.
E-mail address: dyj@dicp.ac.cn (Y.J. Ding).

1381-1169/$ – see front matter © 2008 Elsevier B.V. All rights reserved.
doi:10.1016/j.molcata.2008.10.050

pressed, crushed and sieved to 20–40 mesh particles before it was impregnated with an aqueous solution of $RhCl_3$ (Johnson Matthey) using the incipient wetness method. The Rh loading was 1.0 wt%. After impregnation, the samples were first dried at 373 K for 12 h, then calcined at 673 K for 4 h and finally reduced by H_2 at 673 K for 4 h in a quartz tube. And then the Cl of $RhCl_3$ was completely removed by hot washing and detected by $AgNO_3$. We labeled the obtained samples as Rh/S15 catalyst and kept them in argon atmosphere after drying and reducing.

The above Rh/S15 catalyst was employed as the precursor of PPh_3-Rh/S15 catalyst. The Rh/S15 catalyst was added to a solution of PPh_3 in tetrahydrofuran and stirred for 0.5 h. The solvent was removed under vacuum at room temperature, and the final gray sample was labeled as PPh_3-Rh/S15 catalyst (the molar ratio of P/Rh = 15:1, unless specified) and stored under argon atmosphere.

$HRh(CO)(PPh_3)_3$ was prepared as previously described [10], and dissolved with PPh_3 (the total molar ratio of P/Rh = 15:1) in toluene. Then S15 was introduced into this solution and the mixture was stirred for 0.5 h. Finally the yellow $HRh(CO)(PPh_3)_3$/S15 was obtained after removing toluene.

2.2. Instrumentation

The uptake data of H_2 pulse adsorption was obtained from a Micromeritics ASAP 2010 apparatus. TEM study of powder materials was carried out using a JEOL JEM-2000EX transmission electron microscope operated at 120 kV. Solid-state ^{31}P MAS NMR spectra were recorded at room temperature on a VARIAN Infinity plus spectrometer equipped with a 2.5 mm Chemagnetics wide line probe at a working frequency of 161.8 MHz. The spectra were recorded under a magic angle spinning rate of 12 kHz and the $\pi/4$ pulse was 0.7 u. The spectra were collected after 500 scans using a pulse delay of 3.0 s. All chemical shifts are reported in parts per million (δ) relative to the chemical shifts of 85% H_3PO_4 (^{31}P). X-ray photoelectron spectroscopy (XPS) spectra were recorded by a VG ESCALAB MK-2 X-ray photoelectron spectrometer using Al-Kα (1486.6 eV) as the exciting source. Si_{2p} = 103.4 eV as internal standard for S15 was used to correlate the values of obtained binding energy to normalize the charging effects appearing commonly on such non-conductive samples. In experiments, the samples were pressed into self-supported wafers and mounted on the stainless steel manipulator. Base pressure of the system was 2×10^{-8} Pa. Samples utilized were 3% Rh/S15.

In situ FT-IR spectra were measured by a Bruker EQUINOX 55 single-beam Fourier transform infrared spectrometer equipped with a DTGS detector. All spectra were recorded with 16 scans with a resolution of 4 cm^{-1}. The sample wafer was mounted in a high temperature/high pressure cell (SPECAC INC P/N 5850) fitted with ZnSe windows and an automatic temperature controller; the cell is a water-cooled, stainless steel chamber. The sample was reduced in flowing H_2 at 393 K for 1 h. After reduction, the catalyst was cooled down to 323 K in a flow of N_2 and was subjected to FT-IR measurement (spectrum A). Subsequently, CO was introduced into this system, and kept flowing for 30 min under atmospheric pressure. After purging the chamber with high-purity N_2 for 30 min, spectrum B was recorded. Subtracting spectrum A from spectrum B gave a final FT-IR spectrum.

2.3. Hydroformylation reaction

The hydroformylation reaction was conducted in a fixed-bed reactor of stainless steel with an inner diameter of 4.6 mm. 0.3 g solid catalyst was packed in the reactor and fixed with quartz wool plugs. Before reaction, the system was reduced at 393 K with H_2 (20 ml/min) for 2 h and subsequently with the reaction mixture ($CO:H_2:C_3H_6$ = 1:1:1). GC analysis of the solutions was performed on a HP-6890N gas chromatograph equipped with an FID and a 30-m (0.25 mm id) DB-FFAP capillary column. A Porapak-QS packed column (2 m, 3 mm id) and a TCD was employed on-line for the determination of tail gas.

Table 1
Hydroformylation activity of different catalysts.

Catalyst	TOF[a]	n/i ratio	Selec.
Rh/S15-6.1[b]	2.74	2.6	19.2
PPh_3-Rh/S15-2.2	119	9.9	99.3
PPh_3-Rh/S15-3.8	225	11.8	100
PPh_3-Rh/S15-6.1	245	12.7	100
PPh_3-Rh/S15-8.7	202	11.0	100
$HRh(CO)(PPh_3)_3$/S15-6.1	301	10.7	100

Reaction conditions: T = 393 K, time on stream = 4 h, P = 1.0 MPa and SV = 2000 h^{-1}.
[a] TOF: mol-butyraldehyde/mol-Rh·hour.
[b] Pore sizes in nm are shown as the last numerical value of each sample.

3. Results and discussion

A comparison of $HRh(CO)(PPh_3)_3$-derived homogeneous catalyst [$HRh(CO)(PPh_3)_3$/S15-6.1, S15-6.1 means SBA-15 with a pore size of 6.1 nm], conventional heterogeneous catalyst (Rh/S15-6.1) and PPh_3-Rh/S15-6.1 catalyst for propene hydroformylation in a fixed-bed reactor (Table 1) indicated that the activity (TOF, mol-butyraldehyde/mol-Rh·hour), selectivity, and n/i (normal to iso) ratio of PPh_3-Rh/S15-6.1 were far higher than those of Rh/S15-6.1. Though PPh_3-Rh/S15-6.1 displayed lower TOF than $HRh(CO)(PPh_3)_3$/S15-6.1, it gave higher n/i ratio than $HRh(CO)(PPh_3)_3$/S15-6.1. The n/i ratio is an important parameter in the industrial hydroformylation process, because normal butyraldehyde is the preferential commercial product [11].

To investigate why PPh_3-Rh/S15-6.1 (TOF = 245, n/i = 12.7) gave higher activity and selectivity than PPh_3-Rh/SiO_2 (TOF = 131, n/i = 8.6) even though the walls of S15 and SiO_2 are both amorphous silica, we studied the dependence of catalytic performance on the pore size of S15. Table 1 shows that the catalytic activity and n/i ratio were strongly dependent on the pore size of support and were maximized at about 6.1 nm. Smaller or larger pores were less suitable for propene hydroformylation. The results of H_2-chemisorptions indicated that Rh(0) nano-particles were highly dispersed. The particle diameter of Rh(0) nano-particles supported in S15-2.2, S15-3.8, S15-6.1 and S15-8.7 was 0.9 nm, 1.1 nm, 1.4 nm and 0.9 nm, respectively. Though the Rh(0) nano-particles supported in S15-2.2 and S15-8.7 were similar, PPh_3-Rh/S15-8.7 gave higher activity and selectivity than PPh_3-Rh/S15-2.2. Consequently, there was no evidence of correlation between catalytic activity and Rh(0) nano-particle size.

Fig. 1 shows TEM images of Rh/S15-6.1, PPh_3-Rh/S15-6.1 and HRh $(CO)(PPh_3)_3$/S15-6.1 catalysts. A typical micrograph of the Rh nano-particles was shown in the TEM images of the Rh/S15-6.1 catalyst, the PPh_3-Rh/S15-6.1 catalyst treated by syngas and the PPh_3-Rh/S15-6.1 catalyst after reaction in Fig. 1(a), (b) and (c), respectively. No dramatic differences could be observed among the images of the Rh/S15-6.1 catalyst and the PPh_3-Rh/S15-6.1 catalysts. The results revealed that the Rh nano-particles remained unchanged throughout the preparation and reaction of the PPh_3-Rh/S15-6.1 catalyst, and the PPh_3-Rh/S15-6.1 catalyst was a real heterogeneous catalyst during the reaction. No Rh particle but only the hexagonal structure of the S15 mesoporous molecular sieve was shown in the TEM image of the $HRh(CO)(PPh_3)_3$/S15-6.1 catalyst in Fig. 1(d). Further EDX analysis ascertained the existence of Rh, to be exact, the Rh species in the $HRh(CO)(PPh_3)_3$/S15-6.1 catalyst was Rh^{1+} ion.

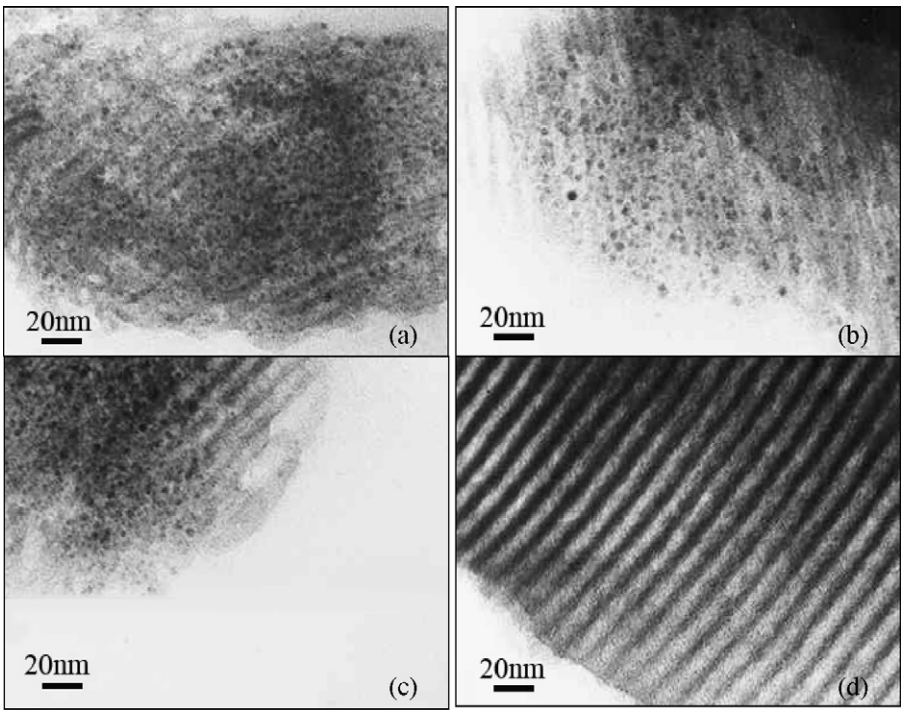

Fig. 1. TEM micrograph of Rh/S15-6.1 (a), PPh_3-Rh/S15-6.1 treated by syngas (b), PPh_3-Rh/S15-6.1 after reaction (c) and $HRh(CO)(PPh_3)_3$/S15-6.1 (d) catalyst.

Surface analysis by XPS spectra was carried out in terms of the binding energy (BE) values of Rh in Fig. 2, after necessary Si_{2p} correction, to study the changes in the chemical states of Rh. The binding energy of Rh 3d5/2 level in the Rh/S15-6.1, Rh/S15-6.1 treated by syngas and PPh_3-Rh/S15-6.1 samples were almost similar at 306.9 eV, which proved essentially that all Rh was present as Rh^0 species. However, $Rh^{\delta+}$ $(0<\delta<1)$ species with the binding energy of 307.7 eV was detected after the PPh_3-Rh/S15-6.1 sample was treated with syngas. It is important to emphasize that $Rh^{\delta+}$ $(0<\delta<1)$ species in situ formed after the PPh_3-Rh/S15-6.1 sample was treated with syngas, which should be an average chemical states of Rh^0 species and Rh^{1+} species. These binding energies were found to be in accord with the literature values [12,13]. Accordingly, the chemical state of Rh changed as follows: the Rh nano-particles were fixed firmly on S15 by Rh–O bonds between Rh and S15 after calcination, then most Rh species could be reduced to Rh^0 species to be the conventional heterogeneous Rh/S15-6.1 catalyst; Rh still kept their Rh^0 species after they had been chemically adsorbed by PPh_3 to become the PPh_3-Rh/S15-6.1 catalyst. Then some Rh^0 species in the PPh_3-Rh/S15-6.1 catalyst were oxidized to Rh^{1+} species by an OH group of the support and CO during the hydroformylation, and bound to the Rh^0 species in nano-particles, and all these Rh species were tightly bound by the very strong Rh–Rh bonds [14]. Therefore, the PPh_3-Rh/S15-6.1 catalyst could largely lessen the metal leaching problem and possessed excellent stability.

The coordination behavior of PPh_3 to Rh was investigated with solid-state ^{31}P MAS NMR spectroscopy. In Fig. 3, the ^{31}P NMR spectra of $HRh(CO)(PPh_3)_3$/S15-6.1 catalyst treated by syngas displayed three resonance peaks at −5.8, +28.9 and +40.9 ppm, which were

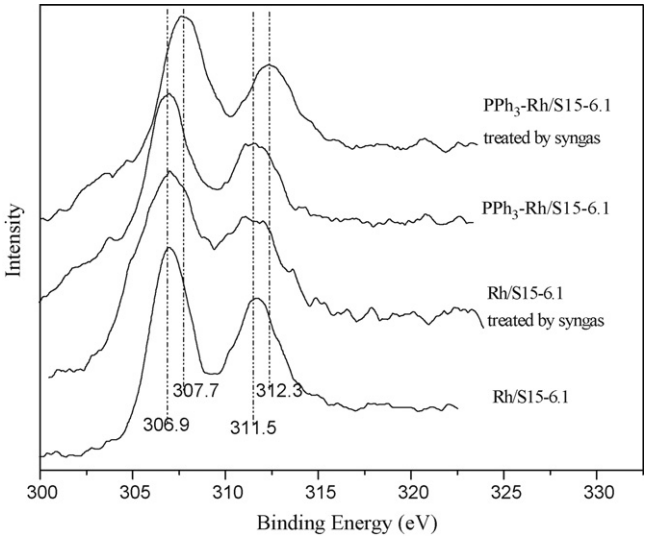

Fig. 2. The Rh 3d5/2 XPS spectra of different catalysts.

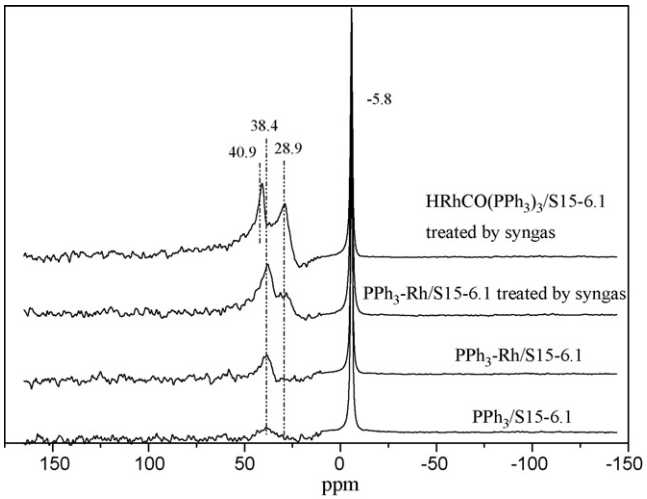

Fig. 3. Solid-state ^{31}P NMR spectra of the catalysts.

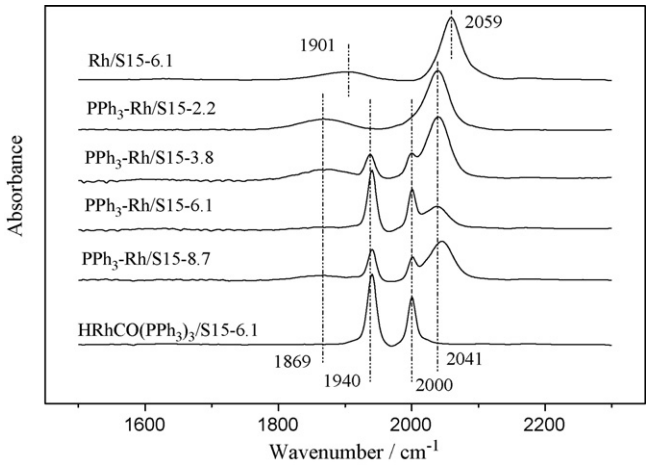

Fig. 4. FT-IR spectra of CO treated catalysts.

attributed to physically adsorbed PPh_3, PPh_3 in a Rh-phosphine carbonyl complex, and PPh_3 in $HRh(CO)(PPh_3)_3$, respectively [15–18]. While the ^{31}P NMR spectra of PPh_3/S15-6.1 and PPh_3-Rh/S15-6.1 displayed two resonance peaks at −5.8 and +38.4 ppm due to physically adsorbed PPh_3 and chemically adsorbed PPh_3, respectively. More chemically adsorbed PPh_3 on PPh_3-Rh/S15-6.1 than on PPh_3/S15-6.1 suggested that some PPh_3 in PPh_3-Rh/S15-6.1 was chemically adsorbed on Rh nano-particles. After PPh_3-Rh/S15-6.1 was treated by syngas ($CO + H_2$), an additional resonance peak appeared at +28.9 ppm that was assigned to the PPh_3 in Rh-phosphine carbonyl complex. Accordingly, we deduced that some chemically adsorbed PPh_3 on the surface of Rh nano-particles coordinated with Rh nano-particles in the atmosphere of syngas to form Rh-phosphine carbonyl complex in situ, which may be responsible for the high activity and selectivity for hydroformylation.

To further verify the structure of Rh-phosphine carbonyl complex on the catalysts, we studied them by in situ FT-IR as shown in Fig. 4. The absorption signals at 2059 and 1901 cm^{-1} in the FT-IR spectrum of Rh/S15-6.1 were assigned to linear adsorbed CO and bridged adsorbed CO on Rh (area ratio is 3:1), respectively [19]. As the chemically adsorbed PPh_3 led to exposed Rh sites more electron-rich, the absorption peaks of linear and bridged CO on PPh_3-Rh/S15-6.1 (1869 and 2041 cm^{-1}) were shifted to lower wave numbers relative to those on Rh/S15-6.1. The FT-IR spectrum of $HRh(CO)(PPh_3)_3$/S15-6.1 characterized the carbonyl stretching bands of $HRh(CO)_2(PPh_3)_2$ with bands at 1940 and 2000 cm^{-1} (area ratio of 10:7), as assigned in the literature [4,20]. The reaction of $HRh(CO)(PPh_3)_3$ with CO produces $HRh(CO)_2(PPh_3)_2$, which exists as two rapidly equilibrating trigonal bipyramidal isomers [21,22]. Interestingly, all CO absorption peaks at 1869, 1940, 2000 and 2041 cm^{-1} coexisted on the FT-IR spectrum of PPh_3-Rh/S15-6.1 with the corresponding ratio of peak areas (1940:2000 = 10:7; 2041:1869 = 3:1). Therefore, it was rational to believe that homogeneous active species similar to $HRh(CO)_2(PPh_3)_2$ were formed in situ on the surface of Rh/S15-6.1 after PPh_3-Rh/S15-6.1 was treated with CO. Thus, characteristics of homogeneous and heterogeneous catalysts were both present on PPh_3-Rh/S15-6.1 at reaction atmosphere. As all FT-IR spectrums recorded the differences of the catalyst before and after CO chemisorption, no Rh–H vibration could be detected.

It is amazing that increased homogeneity of the active species of $HRh(CO)_2(PPh_3)_2$, as indicated by the absorption lines at 1940 and 2000 cm^{-1} in Fig. 4, led to higher activity and larger n/i ratio of PPh_3-Rh/S15 for propene hydroformylation. This further suggested that the $HRh(CO)_2(PPh_3)_2$ active species, formed in situ, were responsible for the high activity and selectivity of PPh_3-Rh/S15. Surprisingly, the amount of $HRh(CO)_2(PPh_3)_2$ species was strongly dependent on the S15 pore size, and was maximized at 6.1 nm.

Three kinds of shape selective catalysis are widely known: reactant, product, and intermediate selectivity. Van Bavel et al. demonstrated that not only the kinetic diameter but also the shape of molecular was an important factor for being able to be adsorbed or formed in the micropores of S15 [23]. In the present reaction, a possible explanation is that the pore size of support may not only affect the amount of active species but also the shape of active species formed inside the pores. Similar to the shape selectivity of reactions occurring in zeolite catalysts, the pore size compatibility of nano-pore materials to ligand coordinated Rh particles is important for the regioselectivity of hydroformylation.

In the case of PPh_3-Rh/S15, the $HRh(CO)_2(PPh_3)_2$ species formed in situ on the Rh nano-particles. This led to a larger steric hindrance on PPh_3-Rh/S15 than on $HRh(CO)(PPh_3)_3$/S15. That is why PPh_3-Rh/S15 produced a higher n/i ratio than $HRh(CO)(PPh_3)_3$/S15.

One more important fact was that the stability of the PPh_3-Rh/S15-6.1 catalyst was much better than that of the $HRh(CO)(PPh_3)_3$/S15-6.1 catalyst as shown in Fig. 5. It is shown that after 100 h of operation, the conversion of propene on the $HRh(CO)(PPh_3)_3$/S15-6.1 catalyst decreased from 41.3 to 14.3% while that of PPh_3-Rh/S15-6.1 catalyst remained unchanged. From the TEM micrograph of Fig. 1, no deposition can be viewed from the image of $HRh(CO)(PPh_3)_3$/S15-6.1, so the homogeneous catalyst must be leached during reaction after 100 h of running. On the other hand, when PPh_3-Rh/S15-6.1 catalyst was employed in hydroformylation of propene, the solution was transparent and colorless, and the evidence obtained from Inductive Coupled Plasma-Atomic Emission Spectroscopy (ICP-AES) measurements showed that no Rh species in excess of 0.01 ppm level was detected in the product solutions, while PPh_3 was found in the GC–MS analysis of the product solution. Therefore, the activity and selectivity of PPh_3-Rh/S15-6.1 catalyst tended to decline after 200 h should not be the result of the lost of Rh species, but the lost of PPh_3. The reason for the deactivation of the PPh_3-Rh/S15 catalyst could be further confirmed by the fact that no sign of deactivation was observed over a period of more than 1000 h on the same series of catalyst supported on SiO_2 on the condition that PPh_3 was added at 300–350 h of time on stream [3]. Thus, the explanation for the excellent stability of PPh_3-Rh/S15 catalyst might be that when the coordination bonds between $Rh^{\delta+}$ and ligands were often broken during catalytic reactions, Rh species were fastened on S15 by the Rh–O bonds and the very strong Rh–Rh

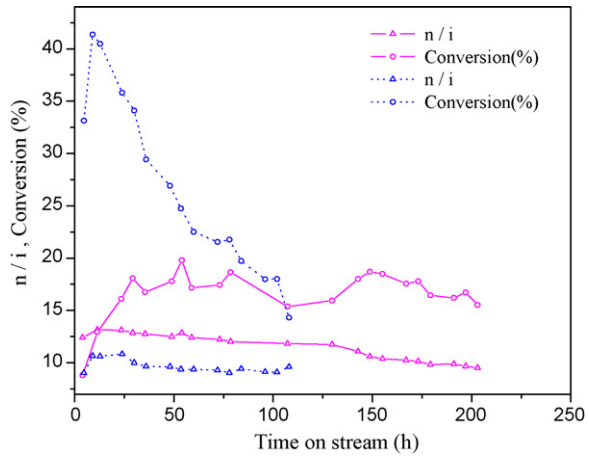

Fig. 5. Comparison of propene hydroformylation over $HRh(CO)(PPh_3)_3$/S15-6.1 (the dot line) catalyst and PPh_3-Rh/S15-6.1 (the solid line) catalyst. Reaction conditions: P = 1.0 MPa, SV = 1500 h^{-1} and T = 393.

bonds, but PPh_3 was inevitably leached in the case of PPh_3-Rh/S15; on the other hand, Cole-Hamilton has reported that the Rh ion may break away from the support in a heterogenized homogeneous catalyst [2]. Consequently, the problem of metal leaching might be greatly suppressed during reaction.

4. Conclusion

The presented work confirmed the in situ formation of homogenous active species on the surface of a heterogeneous catalyst, and the effect of nanometer-sized pores on the in situ formation of $HRh(CO)_2(PPh_3)_2$ active species has been investigated. This development of a new class of easily workable catalyst combines the practical advantages of a heterogeneous catalyst with the efficiency of a homogeneous system.

Acknowledgments

This work is supported by the National Natural Science Foundation of China (20073046) and the Chinese Science and Technology Ministry (Grant No. G2003CB615803). We appreciate Ms. X.W. Han, Prof. D.Y. Zhao and Prof. M. Schlossman for technical support and helpful discussions.

References

[1] C.D. Frohning, C.W. Kohlpaintner, B. Cornils, W.A. Hermann, Applied Homogeneous Catalysis with Organometallic Compounds, vol. 1, Wiley–VCH, Weinheim, 2000, p. 29.
[2] D.J. Cole-Hamilton, Science 299 (2003) 1702–1706.
[3] L. Yan, Y.J. Ding, H.J. Zhu, J.M. Xiong, T. Wang, Z.D. Pan, L.W. Lin, J. Mol. Catal. A: Chem. 234 (2005) 1–7.
[4] H.J. Zhu, Y.J. Ding, L. Yan, Y. Lu, C. Li, X.H. Bao, L.W. Lin, Chem. Lett. 33 (2004) 630–631.
[5] M. Garland, Organometallics 12 (1993) 535–543.
[6] C. Fyhr, M. Garland, Organometallics 12 (1993) 1753–1764.
[7] D.T. Brown, T. Eguchi, B.T. Heaton, J.A. Iggo, R.J. Whyman, Chem. Soc. Dalton Trans. (1991) 677–683.
[8] A.J. Bruss, M.A. Gelesky, G. Machado, J. Dupont, J. Mol. Catal. A: Chem. 252 (2006) 212–218.
[9] D. Zhao, J. Feng, Q. Huo, N. Melosh, G.H. Fredrickson, B.F. Chmelka, G.D. Stucky, Science 279 (1998) 548–552.
[10] D. Evans, G. Yagupsky, G. Wilkinson, J. Chem. Soc. A 11 (1968) 2660–2671.
[11] L.A. Gerritsen, A. Van Meerkerk, M.H. Vreugdenhil, J.J.F. Scholten, J. Mol. Catal. 9 (2) (1980) 139–155.
[12] S. Lars, T. Andersson, M.S. Scurrell, J. Catal. 59 (1979) 340–356.
[13] J.S. Brinen, A. Melera, J. Phys. Chem. 76 (1972) 2525–2526.
[14] L.W. Lin, Y. Kou, M. Zou, Z. Yan, Phys. Chem. Chem. Phys. 3 (2001) 1789–1794.
[15] K. Mukhopadhyay, A.B. Mandale, R.V. Chaudhari, Chem. Mater. 15 (2003) 1766–1777.
[16] C. Bianchini, M. Frediani, F. Vizza, Chem. Commun. (2001) 479–480.
[17] K.J. Stanger, J.W. Wiench, M. Pruski, R.J. Angelici, J. Mol. Catal. A: Chem. 195 (2003) 63–82.
[18] Y.S. Varshavsky, T.G. Cherkasova, I.S. Podkorytov, Inorg. Chem. Commun. 7 (2004) 489–491.
[19] A.C. Yang, C.W. Garland, J. Phys. Chem. 61 (1957) 1504–1512.
[20] A. Riisager, R. Fehrmann, S. Flicker, R. van Hal, M. Haumann, P. Wasserscheid, Angew. Chem. Int. Ed. 44 (2005) 815–819.
[21] C.K. Brown, G. Wilkinson, J. Chem. Soc. A 11 (1970) 2753–2764.
[22] G. Yagupsky, C.K. Brown, G. Wilkinson, J. Chem. Soc. D: Chem. Commun. 21 (1969) 1244–1245.
[23] E. Van Bavel, V. Meynen, P. Cool, K. Lebeau, E.F. ansant, Langmuir 21 (2005) 2447–2453.